Kinetic Analysis of Metal Binding to the Amino-Terminal Domain of ZntA by Monitoring Metal−Thiolate Charge-Transfer Complexes†

Sabari J. Dutta, Junbo Liu, and Bharati Mitra*

Department of Biochemistry and Molecular Biology, School of Medicine, Wayne State University, Detroit, Michigan 48201

Received April 26, 2005; Revised Manuscript Received July 31, 2005

ABSTRACT: ZntA, a P_{1B}-ATPase transporter from *Escherichia coli*, mediates resistance specifically to Pb^{2+}, Zn^{2+}, and Cd^{2+} by active efflux. ZntA has a hydrophilic N-terminal domain that binds one metal ion. This domain, ∼120 residues long, contains the GXXCXXC motif that has been shown to be the binding site for metal ions such as Cu^+ and Zn^{2+} in P_{1B}-type ATPases, and an additional cysteine-rich motif, CCCDGAC. We report here that binding of Pb^{2+} and Cd^{2+} to this domain produces changes in the absorbance spectrum in the 250−400 nm range indicative of metal−thiolate charge-transfer complexes. The spectral changes indicate that only two cysteines are ligands to Cd^{2+}, but three or more cysteines are involved in binding Pb^{2+}; this confirms earlier results that the GXXCXXC sequence is not sufficient to bind Pb^{2+}, which likely involves residues from the CCCDGAC motif. The absorbance changes were used to measure metal binding kinetics of the N-terminal domain using stopped-flow techniques. Binding was described by simple second-order kinetics with a rate constant, k_{on}, of $\sim 10^6-10^7$ M^{-1} s^{-1}, at 4 °C. The activation energy of binding is similar for both Pb^{2+} and Cd^{2+}; however, the entropy change is greater for Pb^{2+}. The surprisingly large rate constant for metal binding to the N-terminal domain of ZntA, compared to its low turnover rate, indicates that this step is not rate limiting in the overall transport mechanism. These results, in conjunction with earlier studies, suggest that metal binding to the transmembrane site in ZntA or metal release from the transporter is the slow step in the reaction cycle.

P-type ATPases catalyze the ATP-dependent translocation of positively charged substrates across membranes (*1*). Their name refers to the formation of an acyl phosphate intermediate during the reaction cycle, when the γ-phosphate of ATP is transferred to a conserved aspartate residue. P_{1B}-type ATPases, a subgroup of this family, transport soft metal ions such as Pb^{2+}, Zn^{2+}, Cd^{2+}, Co^{2+}, Cu^{2+}, Cu^+, and Ag^+ (*2*−*16*). These transporters play important roles in maintaining homeostasis of essential soft metals and also mediate resistance to purely toxic metals in bacteria and plants by active efflux. Humans have two Cu^+-transporting P_{1B}-type ATPases, defects in which cause Menkes' and Wilson's diseases (*6*−*8*). ZntA, the focus of this study, is a P_{1B}-type ATPase from *Escherichia coli* that confers resistance specifically to toxic concentrations of Cd^{2+}, Pb^{2+}, and Zn^{2+}, by transporting these metal ions out of the cytoplasm (*10*−*11*).

Most P_{1B}-type ATPases have a highly conserved hydrophilic soft-metal binding N-terminal domain; this is a feature that distinguishes them from other subgroups of P-type ATPases (*2*−*4*, *17*−*21*). This metal-binding site in P_{1B}-type ATPases that are specific for transporting Cu^+/Ag^+ or $Zn^{2+}/Pb^{2+}/Cd^{2+}$ is made up of the cysteine-containing motif, GXXCXXC, repeated one to six times depending on the particular transporter (*6*−*8*, *22*). The N-terminal domain of ZntA is ∼120 amino acids long and binds a single soft metal ion (*21*). In addition to a single copy of the ^{56}GXXCXXC^{62} motif, it has the motif ^{29}CCX(D/E)XXC^{35}; the latter motif is conserved in a few close homologues of ZntA, notably those from *Salmonella typhi* and *Klebsiella pneumoniae*. The NMR structure of part of the N-terminal domain of ZntA, containing residues 46 to 118, was solved with and without Zn^{2+} bound to it; this protein contained the ^{56}GMDCAAC^{62} motif but lacked the ^{29}CCX(D/E)XXC^{35} sequence (*23*). The Zn^{2+} site was solvent-exposed; Zn^{2+} was bound in tetrahedral coordination to the two Cys residues and the carboxylate oxygens of the Asp residue from the ^{56}GMDCAAC^{62} motif. We recently showed that while the ^{56}GMDCAAC^{62} motif is sufficient for binding Cd^{2+} and Zn^{2+} to the N-terminal domain of ZntA, the binding of Pb^{2+} requires, in addition, the first forty-five residues of ZntA containing the ^{29}CCX(D/E)XXC^{35} motif (*21*).

While it is clear that the N-terminal domain of P_{1B}-type ATPases can bind soft metals with high affinity, its function in the overall transport mechanism is yet to be unequivocally determined. Full-length ZntA has two high-affinity metal binding sites, one in the N-terminal domain, and one in the transmembrane domain (*24*). A mutant of ZntA lacking the N-terminal domain, ΔN-ZntA, as well as a different mutant in which the two cysteines of the ^{56}GMDCAAC^{62} motif were replaced by alanines, C59A/C62A-ZntA, lost the N-terminal metal site and could bind only a single metal ion with high affinity (*24*, *25*). Both mutants were active in vitro and had the same metal specificity as *wt*ZntA, though the catalytic activity was 2−3-fold lower than that of *wt*ZntA for each of

† This work was supported by United States Public Health Service Grant GM-61689 (to B.M.).

* Address correspondence to this author at Department of Biochemistry and Molecular Biology, Wayne State University School of Medicine, 540 E. Canfield Avenue, Detroit, MI 48201. E-mail: bmitra@med.wayne.edu. Phone: (313) 577-0040. Fax: (313) 577-2765.

10.1021/bi050761k CCC: $30.25
Published on Web 10/05/2005

the three substrate metals. Chimeric proteins, in which the N-terminal domain of ZntA was replaced by the corresponding domain from the Wilson's Cu^+ transporter, showed similar behavior (*26*). The same result was also observed in vivo (*21*). A *zntA*-deleted strain carrying the mutant Δ*N-zntA* gene on a plasmid was able to grow in a medium containing Pb^{2+}, Zn^{2+}, and Cd^{2+}, but the growth rate was rather slow, placing it at a significant disadvantage relative to a *zntA*-deleted strain carrying the *wtzntA* gene on a plasmid when exposed to toxic concentrations of Pb^{2+}, Zn^{2+}, and Cd^{2+}. Thus it appears that though the metal-binding site in the N-terminal domain is not essential for in vitro activity, it confers a kinetic advantage on the transporter. ZntA and other P_{1B}-type ATPases have overall catalytic rates that are much slower than P_2- and P_3-type ATPases (*15*, *27*). It is not yet known with certainty which individual step(s) in the overall mechanism of P_{1B}-type ATPases is intrinsically slow. However, earlier work where we monitored the acyl phosphate formation activity of ZntA suggested that metal binding to the transporter, and/or its release, is the slow step (*28*).

In this study, we measured the kinetics of metal binding to the isolated N-terminal domain of ZntA, N1-ZntA.[1] Our hypothesis, supported by the results from the ΔN-ZntA, C59A/C62A-ZntA, and the chimeric mutants, is that the more solvent exposed N-terminal site binds the metal ion to be transported by rapidly exchanging it from tightly bound chaperones and chelators and subsequently passes it to the metal-binding site in the membrane. The metal-binding site in the membrane is able to bind metal ions directly from the cytosol, since ΔN-ZntA and C59A/C62A-ZntA both retain one intact high-affinity metal site, but the process may be less efficient. Thus, the N-terminal domain may act as a covalently attached metal chaperone that binds metal ions from the cytosol and concentrates them locally for faster transfer to the transport domain. The small enhancement of rate due to the N-terminal domain may be crucial for survival of the organism at the metal ion concentrations in its native environment and may have dictated why it has been conserved in many, but not all, P_{1B}-type ATPases.

We took advantage of charge-transfer complexes that are formed when Pb^{2+} and Cd^{2+} bind to N1-ZntA, to measure metal binding rates in a stopped-flow spectrophotometer. These complexes, with distinct absorbance spectra in the 250−400 nm range, as well as peaks with high extinction coefficients, provide an extremely useful intrinsic tool to measure metal binding kinetics using stopped-flow techniques. By measuring the formation of the charge-transfer peaks with time when metal is added to N1-ZntA, we determined that metal binding is described by simple second-order kinetics and the rate constant for metal binding is surprisingly fast, especially in comparison to the low overall catalytic rate of ZntA.

EXPERIMENTAL PROCEDURES

Materials. Standard metal stock solutions were purchased from Sigma. Buffers and water used in these experiments were passed through Chelex 100 (Sigma) to remove extraneous metal salts; the estimated final metal content of buffers was < 50 nM. Buffers were deoxygenated by flushing with argon.

Purification of N1-ZntA. Recombinant N1-ZntA, containing residues 1−111 of ZntA, was expressed in the pET-16b plasmid without any affinity tags and purified as described before (*21*). The concentration of N1-ZntA was determined by using an extinction coefficient of 1.14 $(mg/mL)^{-1}$ at 280 nm, determined from total amino acid hydrolysis (*21*).

Direct and Competition Titration of N1-ZntA with Pb^{2+} and Cd^{2+}. UV−vis studies were carried out in a Varian Cary 1E double beam spectrophotometer. Metal-free, reduced N1-ZntA was prepared by treating 1−2 mg of protein with 2 mM DTT and 5 mM EDTA at 4 °C for 1 h. DTT and EDTA were removed by passage through two consecutive Sephadex G-25 columns. The reduced protein was stored under anaerobic conditions and used within 1−2 h. The reduced state of the protein was confirmed by measuring available free cysteines using a standard titration with 5,5′-dithiobis-(2-nitrobenzoic acid) (DTNB) (*29*). Titration with lead acetate or cadmium chloride was carried out with deoxygenated metal salt and protein solutions under argon at 4 or 22 °C in 10 mM BisTris, pH 7.0. Aliquots of either lead acetate or cadmium chloride solutions were added from a gastight Hamilton syringe to reduced N1-ZntA in a sealed cuvette. Following each addition, the solution was mixed well and the spectrum of the metal-bound protein was collected from 200 to 750 nm. The same aliquots of the metal salt solutions were also added to the reference cuvette in which protein was omitted. The spectrum of apo-N1-ZntA was subtracted from each spectrum recorded; the latter was also corrected for dilution.

Kinetic Analysis of Metal Binding to N1-ZntA. The rate of metal binding to N1-ZntA was measured in a stopped-flow spectrophotometer (Applied Photophysics, SX 18.MV) at 4 °C. Metal-free, reduced N1-ZntA was prepared as described above and loaded in one syringe. The second syringe contained the appropriate concentration of the metal salt solution prepared in metal-free and deoxygenated buffer. The buffer used in all stopped-flow measurements was 10 mM BisTris, pH 7.0. Special care was taken to ensure that the syringes and tubing were completely metal-free before the start of the experiment. The binding of metal to N1-ZntA was measured by monitoring the increase in absorbance at 339 or 255 nm for Pb^{2+} and at 253 nm for Cd^{2+}. The data were fitted to single and double exponential fits when the conditions were pseudo-first-order with the concentration of one reactant greater than 5-fold that of the other. The data were also fitted by numerical integration to a simple second-order equation using the Pro/K software supplied by Applied Photophysics.

The dependence of initial rates on the concentration of metal salts was measured by varying the metal salt solution at a fixed protein concentration. Similarly, the dependence of initial rates on the concentration of N1-ZntA was measured by varying the protein concentration at a fixed metal salt concentration. Initial rates were calculated from the data in the range where the concentrations of both protein and metal ion were constant, and no significant amount of the complex had accumulated.

The temperature dependence of the binding of metal salts to N1-ZntA was measured by varying the temperature from

[1] Abbreviations: DTNB, 5,5′-dithiobis(2-nitrobenzoic acid); EDTA, ethylenediaminetetraacetic acid; N1-ZntA, residues 1−111 of ZntA; SDS−PAGE, sodium dodecyl sulfate polyacrylamide gel electrophoresis.

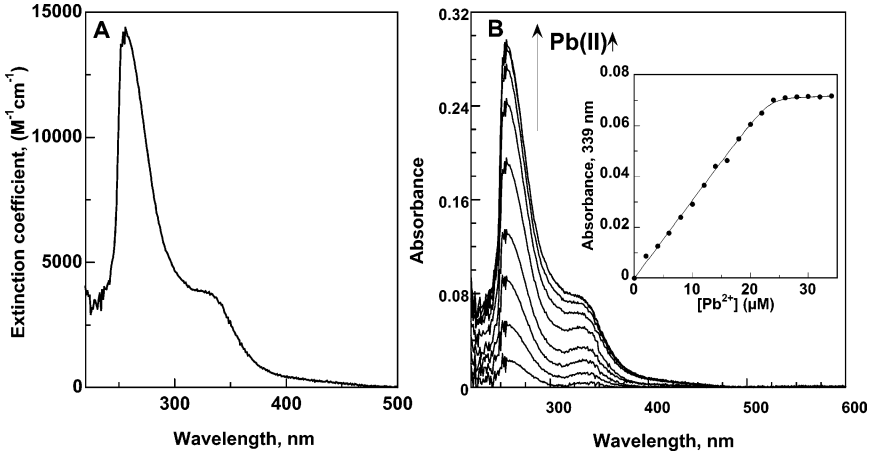

FIGURE 1: (A) Absorbance spectrum of the complex between N1-ZntA and lead acetate in 10 mM BisTris, pH 7.0 and 20 °C. The spectrum due to metal-free, reduced N1-ZntA alone has been subtracted. (B) Spectra obtained during titration of 20 μM N1-ZntA with increasing concentrations of lead acetate in 10 mM BisTris, pH 7.0 and 20 °C. The spectrum of metal-free, reduced N1-ZntA was subtracted from each spectrum. The inset shows the absorbance changes at 339 nm as a function of the added lead salt concentration. The data were fitted to eq 1.

4 °C to 20 °C. The same protein and metal concentrations were used at the different temperatures; the metal concentration was ~5-fold the protein concentration.

RESULTS

Pb^{2+}-Thiolate and Cd^{2+}-Thiolate Charge-Transfer Complexes on Metal Binding to N1-ZntA. N1-ZntA can bind a variety of heavy metal ions, including Pb^{2+}, with a stoichiometry of one (*21*). When Pb^{2+} binds to N1-ZntA, intense lead−thiolate charge-transfer bands are observed at 255 and 339 nm that reflect the N1-ZntA·Pb^{2+} complex (Figure 1A) (*30*−*33*).

$$\text{N1-ZntA} + Pb^{2+} \leftrightarrow \text{N1-ZntA}\cdot Pb^{2+}$$

The charge-transfer peaks at 255 and 339 nm were useful for measuring the relative affinity of Pb^{2+} for N1-ZntA. A titration of N1-ZntA with increasing concentrations of lead acetate is shown in Figure 1B. The data were fitted to the following equation that assumes a 1:1 binding model (inset, Figure 1B):

$$K_{Pb} = \frac{[\text{N1-ZntA}\cdot Pb^{2+}]}{[\text{N1-ZntA}_{(free)}][Pb^{2+}{}_{(free)}]} \quad (1)$$

where K_{Pb} = association constant of N1-ZntA and Pb^{2+} and [N1-ZntA·Pb^{2+}] = concentration of the complex obtained from the increase in absorbance and extinction coefficient at 255 nm following each addition of Pb^{2+},

$$[\text{N1-ZntA}_{(free)}] = [\text{N1-ZntA}]_{total} - [\text{N1-ZntA}\cdot Pb^{2+}]$$

$$[Pb^{2+}{}_{(free)}] = [Pb^{2+}]_{total} - [\text{N1-ZntA}\cdot Pb^{2+}] - [\text{BisTris}\cdot Pb^{2+}]$$

BisTris was chosen as a buffer because it forms a stable and soluble complex with Pb^{2+} and prevents formation of lead oxide and other insoluble species (*34*). The association constant for the binding of Pb^{2+} to BisTris is 20 893 M^{-1}; this value was used to calculate the free Pb^{2+} concentration in the fit of the data in Figure 1B (inset) (*35*). An association constant of $2.8 \pm 0.9 \times 10^9$ M^{-1} was calculated for the binding of N1-ZntA to Pb^{2+}, in 10 mM BisTris, pH 7.0, and at room temperature.

Binding of Cd^{2+} to N1-ZntA also produces UV−vis spectral changes with a peak centered at ~253 nm (Figure 2A). By titrating N1-ZntA with increasing concentrations of Cd^{2+}, we measured an association constant for the binding of Cd^{2+} to N1-ZntA, $6.4 \pm 4.3 \times 10^7$ M^{-1} in 10 mM BisTris, pH 7.0, at room temperature (Figure 2B). The association constant for the binding of Cd^{2+} for BisTris, 295 M^{-1}, was used to calculate the free Cd^{2+} concentration in fitting the data in Figure 2B (inset) (*35*).

The affinity of Pb^{2+} and Cd^{2+} for N1-ZntA was also determined at 4 °C by direct titration. We obtained association constants of 2.3×10^9 and 5.1×10^7 M^{-1} for the binding of Pb^{2+} and Cd^{2+}, respectively, at 4 °C; these values are not significantly different from those at 20 °C.

The Rate of Binding of Metal Ions to N1-ZntA Using Stopped-Flow Kinetics. Using the changes in absorbance produced when Pb^{2+} and Cd^{2+} bind to N1-ZntA, we measured the rates of metal binding using stopped-flow kinetics. Figure 3A shows the changes in absorbance produced at 255 nm upon addition of a 5-fold molar excess of Pb^{2+} to N1-ZntA at 4 °C in 10 mM BisTris, pH 7.0. The data fit well to a two-exponential equation describing pseudo-first-order kinetics; however, the amplitude of the smaller initial rate was such that it accounted for less than 3% of the total absorbance change. It was, therefore, not considered significant. The fit of the data yielded an observed rate of 481 s^{-1}.

Figure 3B shows the change in absorbance produced at 253 nm upon addition of 5 equiv of Cd^{2+} to N1-ZntA at 4 °C in 10 mM BisTris, pH 7.0. As the figure indicates, these data also fit well to a two-exponential equation; the amplitude of the smaller initial rate was such that it accounted for ~5% of the total change in absorbance. The fit yielded an observed rate of 299 s^{-1}.

Dependence of Initial Rates on Protein and Metal Ion Concentrations. The initial rates for binding of metal ion to

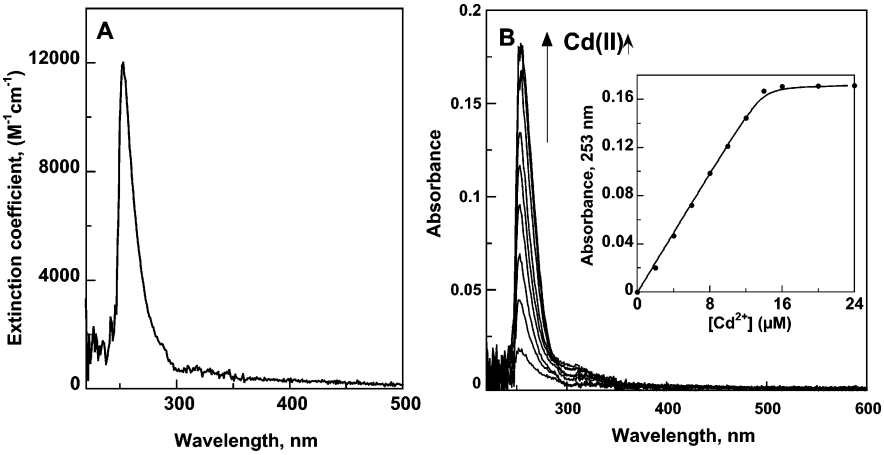

FIGURE 2: (A) Absorbance spectrum of the complex between N1-ZntA and cadmium chloride in 10 mM BisTris, pH 7.0 and 20 °C. The spectrum due to N1-ZntA alone has been subtracted. (B) Spectra obtained during titration of 20 μM N1-ZntA with increasing concentrations of cadmium chloride in 10 mM BisTris, pH 7.0 and 20 °C. The spectrum of N1-ZntA was subtracted from each spectrum. The inset shows the absorbance changes at 253 nm as a function of the added cadmium salt concentration. The data were fitted to eq 1.

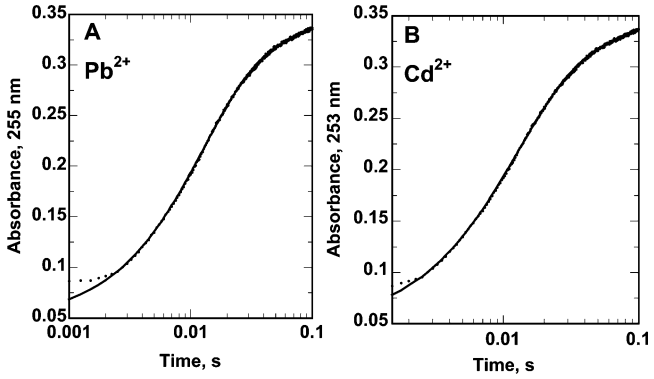

FIGURE 3: Changes in absorbance with time when 5 equiv of (A) lead acetate or (B) cadmium chloride was added to reduced, metal-free N1-ZntA under anaerobic conditions in 10 mM BisTris, pH 7.0, at 4 °C. The concentration of N1-ZntA used was (A) 12.7 μM or (B) 11.2 μM. The lines represent two-exponential fits to the data starting from 2 ms.

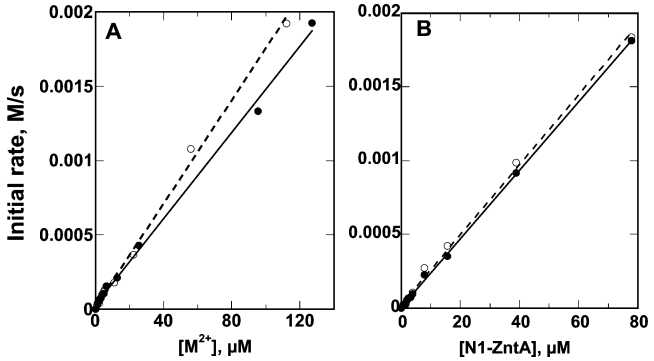

FIGURE 4: (A) Dependence of the initial rate of binding Pb^{2+} (●) and Cd^{2+} (○) on the metal ion concentration at 4 °C. The concentration of N1-ZntA was kept fixed at 12.7 and 11.2 μM for Pb^{2+} and Cd^{2+}, respectively. (B) Dependence of the initial rate of binding Pb^{2+} (●) and Cd^{2+} (○) on the protein concentration at 4 °C. The concentrations of Pb^{2+} and Cd^{2+} were kept fixed at 7.8 μM in both cases.

N1-ZntA increased linearly with metal ion concentrations at a fixed protein concentration (Figure 4A). The initial rates also showed a linear dependence on protein concentration at fixed metal concentrations (Figure 4B). Thus, binding of Pb^{2+} and Cd^{2+} to N1-ZntA is simple first order in each protein and metal ion concentration. Therefore, the metal binding kinetic data can be described by a simple second-order equation:

$$\text{N1-ZntA} + \text{M}^{2+} \underset{k_{on}}{\overset{k_{off}}{\rightleftharpoons}} \text{N1-ZntA}\cdot\text{M}^{2+} \qquad (2)$$

The rate constants, k_{on}, for the binding of Pb^{2+} and Cd^{2+} were determined from the initial rate data in Figure 4. In addition, k_{on} was also determined by fitting the kinetic data to eq 2 directly, using numerical integration software (Pro/K) supplied by Applied Photophysics. The numerical integration method also gave rise to excellent fits as judged by plots of residuals (data not shown). The values obtained for k_{on} for Pb^{2+} and Cd^{2+} were ~6 and 4 × 10^6 M^{-1} s^{-1}, respectively.

Temperature Dependence of the Reaction Rates. To obtain activation energy parameters for the binding of metal ions to N1-ZntA, we measured the rates of Pb^{2+} and Cd^{2+} binding to N1-ZntA at different temperatures ranging from 4 to 20 °C. For these experiments, the metal was in 5-fold excess over the protein concentration. The data were fitted either to a two-exponential equation, assuming pseudo-first-order conditions, or directly to the second-order eq 2, as described above. Both fits yielded similar values of k_{on}. As shown in Figure 5A, k_{on} increases with temperature for the binding of both Pb^{2+} and Cd^{2+}. The data from Figure 5A was replotted as ln(k/T) versus 1/T (Figure 5B) and fitted to a linear form of the Eyring equation,

$$k_{on} = (k_B/h)T \exp(\Delta S^{\ddagger}/R) \exp(-\Delta H^{\ddagger}/RT)$$

where k_B, the Boltzmann constant, equals 1.38 × 10^{-16} erg·K^{-1}; h, Planck's constant, equals 6.624 × 10^{-27} erg·s; and R is the gas constant. $\Delta S^{\ddagger}$ and $\Delta H^{\ddagger}$, the changes in entropy and enthalpy, were calculated from the intercept and slope of the ln(k/T) versus 1/T plot, respectively. The activation energy, $\Delta G^{\ddagger}$, at 25 °C, was calculated from the relationship

$$\Delta G^{\ddagger} = \Delta H^{\ddagger} - T\Delta S^{\ddagger}$$

At 25 °C, $\Delta H^{\ddagger}$ and $\Delta S^{\ddagger}$ for k_{on} were 18.1 kJ/mol and −48.4 J/(K·mol), respectively, for the binding of Pb^{2+} to N1-ZntA. The corresponding $\Delta H^{\ddagger}$ and $\Delta S^{\ddagger}$ for the binding of Cd^{2+} to

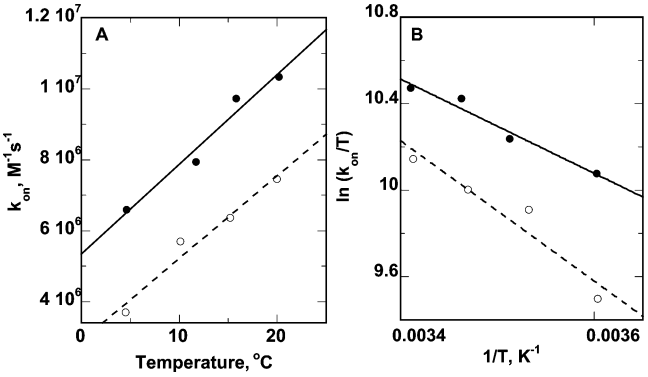

FIGURE 5: (A) Temperature dependence of the rate constant for binding, k_{on}, for Pb^{2+} (●) and for Cd^{2+} (○) to N1-ZntA in 10 mM BisTris, pH 7.0. The protein concentrations used in this experiment were 20.4 and 24.2 μM for Pb^{2+} and Cd^{2+}, respectively; the concentrations of Pb^{2+} and Cd^{2+} were 100 and 120 μM, respectively. (B) Replot of the data from panel A as $\ln(k/T)$ vs $1/T$.

N1-ZntA were 27 kJ/mol and − 20.7 J/(K·mol), respectively. From these values, we calculated $\Delta G^{\ddagger}$ values of 32.5 and 33.2 kJ/mol for the binding of Pb^{2+} and Cd^{2+}, respectively, to N1-ZntA at 25 °C.

DISCUSSION

The function of the N-terminal metal-binding site in P_{1B}-type ATPases in the mechanism of metal transport is not yet clear. It may have a regulatory role in P_{1B}-type ATPases that have multiple metal binding sites in the N-terminal domain, for example, the Wilson's Cu^{+}-ATPase (*36*). However, a negative regulatory role is unlikely for ZntA and homologues with a single metal-binding site in the N-terminal domain, given that when this domain is deleted, the in vitro activity becomes slightly less while the specificity is unchanged, as shown by the ΔN-ZntA mutant (*25*). Rather, the presence of this domain increases the overall activity of the transporter. In the related P_2-type Ca^{2+}-ATPase from sarcoplasmic reticulum, SERCA1, there are two Ca^{2+} binding sites, both located in the transmembrane domain (*37*). Ca^{2+} binds to site 1 first and then moves to site 2. It is possible that the N-terminal metal-binding site in ZntA mechanistically corresponds to site1 in SERCA1: the metal ion would bind rapidly to the N-terminal site and then be transferred to the transmembrane site.

Metal−thiolate charge-transfer spectra are produced upon metal binding to N1-ZntA. A comparison of the spectrum of Pb^{2+}-bound N1-ZntA reported here to those reported for model four-residue peptides containing two to four cysteine residues suggests that, in the Pb^{2+}−N1-ZntA complex, Pb^{2+} is coordinated to more than two cysteine residues (*30*). Pb^{2+} bound to the model peptide CCHH, in a S_2N_2 coordination, showed absorbance maxima at ∼253 and 310 nm; the extinction coefficient at 253 nm was ∼7000 M^{-1} cm^{-1} (*30*). On the other hand, Pb^{2+} bound to the model peptides CCHC and CCCC, in S_3N and S_4 coordination, respectively, showed absorbance maxima at ∼255 and 335 nm; the extinction coefficient at 255 nm was ∼ 14 000−16 000 M^{-1} cm^{-1}. The Pb^{2+}−N1-ZntA complex shows peaks at 255 and 339 nm; also, the extinction coefficient at 255 nm is ∼14 375 M^{-1} cm^{-1}. Thus the spectrum of Pb^{2+}−N1-ZntA resembles that of the Pb^{2+}-bound CCHC and CCCC peptides, and not the CCHH peptide. Therefore, three or more cysteines in N1-ZntA are likely to be involved in binding Pb^{2+}. The signature metal-binding motif of P_{1B}-type ATPases, GMDCAAC, contains only two cysteine residues. The only other cysteine residues in N1-ZntA are part of the ^{29}CCCDGAC^{35} sequence. We have recently shown that the first forty-five residues of ZntA including this sequence are required for binding of Pb^{2+} to N1-ZntA, but not Zn^{2+} or Cd^{2+} (*21*). Taken together, these results strongly suggest that one or more cysteines from the ^{29}CCCDGAC^{35} sequence acts as ligands for Pb^{2+} in addition to the cysteines in the GMDCAAC motif.

The binding of Cd^{2+} to thiolates in peptides also produces charge-transfer complexes, though with single absorbance peaks at wavelengths around 250 nm. Binding of Cd^{2+} to N1-ZntA resulted in an absorbance spectrum with a peak centered at ∼253 nm. The extinction coefficient of this peak (∼12 000 M^{-1} cm^{-1}) suggests that only two sulfurs are directly coordinated with Cd^{2+}; it has been observed that the extinction coefficient due to each Cd−S charge-transfer complex is 5000−6000 M^{-1} cm^{-1} and that the effect is additive (*33*, *38*, *39*). The NMR structure of residues 46−118 of ZntA showed that the ligands for the bound Zn^{2+} are the two cysteines and the aspartate of the GMDCAAC motif (*23*). It appears that Cd^{2+} is bound in an identical manner to N1-ZntA, while the ligands and perhaps coordination geometry of Pb^{2+} binding to N1-ZntA are somewhat different. We did not observe any changes in the difference absorbance spectrum on binding Zn^{2+} to N1-ZntA at ≥220 nm; generally, Zn^{2+} forms charge-transfer complexes with thiolates with peaks at wavelengths <220 nm.

We took advantage of the changes in absorbance upon binding Pb^{2+} and Cd^{2+} to N1-ZntA to obtain quantitative information about the affinity and kinetics of metal binding. The affinity of the protein for Pb^{2+} or Cd^{2+} could be measured by monitoring the changes in the 250−400 nm range following direct titration of N1-ZntA with these metals. The association constants obtained for Pb^{2+} and Cd^{2+} in this study are similar to those we obtained earlier using a competition titration method with a metal indicator, mag-fura-2, though the affinity for Pb^{2+} is slightly higher.

More importantly, the spectroscopic signals produced upon binding of Pb^{2+} and Cd^{2+} to N1-ZntA were useful for measuring metal-binding kinetics. Binding of metal to N1-ZntA was described by simple second-order kinetics, yielding values of the second-order rate constant, k_{on}, of ∼10^6−10^7 M^{-1} s^{-1} for both metals at 4 °C. These k_{on} values are surprisingly large, given that the highest overall catalytic rate of ZntA is 1 s^{-1} at 37 °C; other P_{1B}-type ATPases have been reported to have rates that are even slower (*27*, *15*). It is possible that the rates may be slower when the N-terminal domain is part of the full-length ZntA; this possibility will be tested in the future. However, given the large k_{on} values, it seems unlikely that the rate-limiting step for the transporter is metal binding to the N-terminal site, even when it is part of the full-length ZntA. The rate-limiting step for ZntA and related transporters could possibly be metal binding to the transmembrane site, either by metal transfer from the N-terminal site or by direct binding from the cytosol when the N-terminal domain is missing; it is also possible that metal release from the transporter may be rate-limiting. The observation that the overall catalytic rate of ΔN-ZntA, a mutant of ZntA lacking the N-terminal domain, is 2−3-fold lower compared to full-length ZntA suggests that the rate

of metal transfer from the N-terminal site to the transmembrane site is 2−3-fold faster relative to the rate of direct metal binding to the transmembrane site from the cytosol (*25*). This implies that though metal binding to the N-terminal site is extremely fast, metal transfer from this site to the transmembrane site is slow by many orders of magnitude. Metal transfer from the N-terminal to the membrane site is highly possible since the affinity of the two sites for metal ions is of similar magnitude (*24*).

It should be noted that our measurements were made in a buffer of low ionic strength and relatively low metal affinity. This is unlikely to be the case in vivo, where metals ions are typically part of high-affinity complexes. It is possible that the rate of metal binding to the amino-terminal domain is slower in vivo.

Using the measured values of k_{on} and the association constant, K_a, together with the relationship, $K_a = k_{on}/k_{off}$, we can calculate the rate constant for dissociation of the metal from the N1-ZntA·M^{2+} complex, k_{off}, for Pb^{2+} and Cd^{2+} in 10 mM BisTris, to be $\sim 2 \times 10^{-3}$ and ~ 0.1 s^{-1}, respectively, at 4 °C. Therefore, the rate of dissociation of the N1-ZntA·M^{2+} complex is extremely slow under the experimental conditions. It is possible that release of metal ion from the N-terminal site to the transmembrane site may be faster since the affinity of the transmembrane site for metal is similar to that of the N-terminal site (*24*). However, the slow release rates suggest that, in P_{1B}-type ATPases, slow turnover rates may be a consequence of slow metal transfer rates between two sites and/or slow metal release rates on the periplasmic side. Thus the slow turnover rates for soft-metal transporters may be the price paid for unidirectional transport.

Temperature dependence of the binding of both Pb^{2+} and Cd^{2+} to N1-ZntA reveals that metal binding has an activation energy of ∼33 kJ/mol at 25 °C. This activation energy is primarily enthalpy-driven for Cd^{2+}; the entropy term has a small contribution. However, for Pb^{2+}, the entropy change is much larger and contributes ∼14 kJ/mol to the free energy change. Metal binding leads to a more ordered state, giving rise to the negative entropy term. The larger entropy change term for Pb^{2+} supports other data that suggest its binding is somewhat different from Cd^{2+}: Interestingly, the stability of the complexes of N1-ZntA with Pb^{2+} and Cd^{2+}, as revealed by the association constants obtained by direct titration, is similar at 4 and 20 °C. Since k_{on} increases with temperature, k_{off} must also increase with temperature in a compensatory manner.

Conclusion. In this study, we show that when Pb^{2+} and Cd^{2+} bind to the isolated N-terminal domain of ZntA, absorbance changes occur in the 250−400 nm range, indicative of charge-transfer complexes of these metal ions with thiolates from cysteine residues. These charge-transfer complexes have large extinction coefficients and provide a useful intrinsic tool to study metal binding. The affinity of the N-terminal domain for Pb^{2+} and Cd^{2+} was measured by direct titration by monitoring these absorbance changes. The kinetics of Pb^{2+} and Cd^{2+} binding was determined by monitoring the appearance of the charge transfer peaks with time in a stopped-flow spectrophotometer. Binding was described by second-order kinetics, with a surprisingly large rate constant for binding, k_{on}, of $\sim 10^6-10^7$ M^{-1} s^{-1}. The activation energy of binding is similar for both Pb^{2+} and Cd^{2+}; however, binding of Pb^{2+} results in a greater entropy change. The large rate constant for metal binding to the N-terminal domain of ZntA indicates that this step is not rate limiting in the overall transport mechanism; rather, binding and/or release of metal to the transmembrane site may be quite slow.

ACKNOWLEDGMENT

We are grateful to Dr. Asteriani R. Dewanti for her help with preliminary stopped-flow experiments.

REFERENCES

1. Inesi, G. (1985) Mechanism of calcium transport, *Annu. Rev. Physiol. 47*, 573−601.
2. Lutsenko, S., and Kaplan, J. H. (1995) Organization of P-type ATPases: Significance of Structural Diversity, *Biochemistry 34*, 15607−15613.
3. Solioz, M., and Vulpe, C. (1996) CPx-type ATPases: a class of P-type ATPases that pump heavy metals, *Trends Biochem. Sci. 21*, 237−241.
4. Axelson, K. B., and Palmgren, M. G. (1998) Evolution of Substrate Specificities in the P-Type ATPase Superfamily, *J. Mol. Evol. 46*, 84−101.
5. Nucifora, G., Chu, L., Misra, T. K., and Silver, S. (1989) Cadmium resistance from *Staphylococcus aureus* plasmid pI258 cadA gene results from a cadmium-efflux ATPase, *Proc. Natl. Acad. U.S.A. 86*, 3544−3548.
6. Mercer, J. F., Livingston, J., Hall, B., Paynter, J. A., Begy, C., Chandrasekharappa, S., Lockhart, P., Grimes, A., Bhave, M., Siemieniak, D., et al. (1993) Isolation of a partial candidate gene for Menkes disease by positional cloning, *Nat. Genet. 3*, 20−25.
7. Vulpe, C., Levinson, B., Whitney, S., Packman, S., and Gitschier, J. (1993) Isolation of a candidate gene for Menkes disease and evidence that it encodes a copper-transporting ATPase, *Nat. Genet. 3*, 7−13.
8. Bull, P. C., Thomas, G. R., Rommens, J. M., Forbes, J. R., and Cox, D. W. (1993) The Wilson disease gene is a putative copper transporting P-type ATPase similar to the Menkes gene, *Nat. Genet. 5*, 327−337.
9. Odermatt, A., Suter, H., Krapf, R., and Solioz, M. (1993) Primary Structures of Two P-type ATPases Involved in Copper Resistance in *Enterococcus hirae*, *J. Biol. Chem. 268*, 12775−12779.
10. Rensing C., Mitra B., and Rosen B. P. (1997) The *znt*A gene of *Escherichia coli* encodes a Zn^{2+}-translocating P-type ATPase, *Proc. Natl. Acad. Sci. U.S.A. 94*, 14326−14331.
11. Rensing, C., Sun, Y., Mitra, B., and Rosen, B. P. (1998) Pb^{2+}-translocating P-type ATPases, *J. Biol. Chem. 273*, 32614−32617.
12. Rutherford, J. C., Cavet, J. S., and Robinson, N. (1999) Cobalt-dependent Transcriptional Switching by a Dual-effector MerR-like Protein Regulates a Cobalt-exporting Variant CPx-type ATPase, *J. Biol. Chem. 274*, 25827−2832.
13. Gupta, A., Matsui, K., Lo, J. F., and Silver, S. (1999) Molecular basis for resistance to silver cations in *Salmonella*, *Nat. Med. 5*, 183−188.
14. Rensing, C., Fan, B., Sharma, R., Mitra, B., and Rosen, B. P. (2000) CopA: an *Escherichia coli* Cu(I)-translocating P-type ATPase, *Proc. Natl. Acad. Sci. U.S.A. 97*, 652−656.
15. Mandal, A. K., Cheung, W. D., and Arguello, J. M. (2002) Characterization of a thermophilic P-type Ag^+/Cu^+-ATPase from the extremophile *Archaeoglobus fulgidus*, *J. Biol. Chem. 277*, 7201−7208.
16. Mana-Capelli, S., Mandal, A. K., and Arguello, J. M. (2003) *Archaeoglobus fulgidus* CopB is a thermophilic Cu^{2+}-ATPase: functional role of its histidine-rich-N-terminal metal binding domain, *J. Biol. Chem. 278*, 40534−40541.
17. Lutsenko, S., Petrukhin, K., Cooper, M. J., Gilliam, C. T., and Kaplan, J. H. (1997) N-terminal domains of human copper-transporting adenosine triphosphatases (the Wilson's and Menkes disease proteins) bind copper selectively in vivo and in vitro with stoichiometry of one copper per metal-binding repeat, *J. Biol. Chem. 272*, 18939−18944.
18. DiDonato, M., Narindrasorasak, S., Forbes, J. R., Cox, D. W., and Sarkar, B. (1997) Expression, purification, and metal binding properties of the N-terminal domain from the Wilson disease putative copper-transporting ATPase (ATP7B), *J. Biol. Chem. 272*, 33279−33282.

19. Cobine, P. A., George, G. N., Winzor, D. J., Harrison, M. D., Mogahaddas, S., and Dameron, C. T. (2000) Stoichiometry of complex formation between Copper(I) and the N-terminal domain of the Menkes protein, *Biochemistry 39*, 6857−6863.
20. Ralle, M., Lutsenko, S., and Blackburn, N. J. (2003) The Menkes Disease Protein Binds Copper via Novel 2-coordinate Cu^{+}-Cysteinates in the N-Terminal Domain, *J. Biol. Chem. 278*, 23163−23170.
21. Liu, J., Stemmler, A. J., Fatima, J., and Mitra, B. (2005) Metal-binding characteristics of the amino-terminal domain of ZntA: Binding of Lead is different compared to Cadmium and Zinc, *Biochemistry 44*, 5159−5167.
22. Arguello, J. M. (2003) Identification of ion-selectivity determinants in heavy-metal transport P1B-type ATPases, *J. Membr. Biol. 195*, 93−108.
23. Banci, L., Bertini, I., Ciofi-Baffoni, S., Finney, L. A., Outten, C. E., and O'Halloran, T. V. (2002) A new zinc-protein coordination site in intracellular metal trafficking: solution structure of the Apo and Zn(II) forms of ZntA(46-118), *J. Mol. Biol. 323*, 883−897.
24. Liu, J., Dutta, S. J., Stemmler, A. J., and Mitra, B. (2005) Metal-binding affinity of the transmembrane site in ZntA: implications for metal selectivity, submitted.
25. Mitra, B., and Sharma, R. (2001) The cysteine-rich amino-terminal domain of ZntA, a Pb(II)/Cd(II)/Zn(II)-translocating ATPase from *Escherichia coli*, is not essential for its function, *Biochemistry 40*, 7694−7699.
26. Hou, Z.-J., Narindrasorasak, S., Bhushan, B., Sarkar B., and Mitra, B. (2001) Functional analysis of chimeric proteins of the Wilson Cu(I)-transporting ATPase (ATP7B) and ZntA, a Pb(II)/Zn(II)/Cd(II)-translocating ATPase from *Escherichia coli*, *J. Biol. Chem. 276*, 40858−40863.
27. Sharma, R., Rensing, C., Rosen, B. P., and Mitra, B. (2000) The ATP hydrolytic activity of purified ZntA, a $Pb^{2+}/Cd^{2+}/Zn^{2+}$-translocating ATPase from *Escherichia coli*, *J. Biol. Chem. 275*, 3873−3878.
28. Hou, Z., and Mitra, B. (2003) Characterization of the metal specificity of ZntA from *Escherichia coli* using the acylphosphate intermediate, *J. Biol. Chem. 278*, 28455−28461.
29. Riddles, P. W., Blakeley, R. L., and Zerner, B. (1979) Ellman's reagent: 5,5′-dithiobis(2-nitrobenzoic acid)—a reexamination, *Anal. Biochem. 94*, 75−81.
30. Payne, J. C., Horst, M. A., and Godwin, H. A. (1999) Lead Fingers: Pb^{2+} Binding to structural Zinc-Binding Domains determined Directly by Monitoring Lead-Thiolate Charge-transfer Bands, *J. Am. Chem. Soc. 121*, 6850−6855.
31. Vasek, M., Kagi, J. H. R., and Hill, H. A. O. (1981) Zinc(II), cadmium(II), and mercury(II) thiolate transitions in metallothionein, *Biochemistry 20*, 2852−2856.
32. Fleissner, G., Reigle, M. D., O'Halloran, T. V., and Spiro, T. G. (1998) UVRR Spectroscopy of the Metal Receptor Site in MerR, *J. Am. Chem. Soc. 120*, 12690−12691.
33. Busenlehner, L. S., Cosper, N. J., Rosen, B. P., Wong, M. D., and Giedroc, D. P. (2001) Spectroscopic properties of the metalloregulatory Cd(II) and Pb(II) sites of S. aureus pI258 CadC, *Biochemistry 40*, 4426−4436.
34. Vallee, B. L., and Wacker, W. E. C. (1970) Metalloproteins, *The Proteins Vol. V*, Academic Press, New York, London.
35. Scheller, K. H., Abel, T. H. J., Polanyi, P. E., Wenk, P. K., Fischer, B. E., and Sigel, H. (1980) Metal Ion/Buffer Interactions, *Eur. J. Biochem. 107*, 455−466.
36. Tsivkovskii, R., MacArthur, B. C., and Lutsenko, S. (2001) The Lys1010-Lys1325 fragment of the Wilson's disease protein binds nucleotides and interacts with the N-terminal domain of this protein in a copper-dependent manner, *J. Biol. Chem. 276*, 2234−4233.
37. Toyoshima, C., and Inesi, G. (2004) Structural Basis of Ion Pumping by Ca^{2+}-ATPase of the Sarcoplasmic Reticulum, *Annu. Rev. Biochem. 73*, 269−292.
38. Henehan, C. J., Pountney, D. L., Zerbe, O., and Vasek, M. (1993) Identification of cysteine ligands in metalloproteins using optical and NMR spectroscopy: cadmium-substituted rubredoxin as a model $[Cd(CysS)_4]^{2-}$ center, *Protein Sci. 2*, 1756−1764.
39. Pountney, D. L., Tiwari, R. P., and Egan, J. B. (1997) Metal- and DNA-binding properties and mutational analysis of the transcription activating factor, B, of coliphage 186: a prokaryotic C4 zinc-finger protein, *Protein Sci. 6*, 892−902.

BI050761K